Processing and Application of Ceramics 19 [1] (2025) 57–64
https://doi.org/10.2298/PAC2501057S

Study on the microstructure, dielectric properties and phase transition behaviour of $MgTiO_3$ and $Ca_{0.61}La_{0.26}TiO_3$ mixed-phase ceramics

Chun-Hsu Shen[1], Yih-Chien Chen[2], Chung-Long Pan[3,*]

[1]*Department of Electronic Engineering, Ming Chuan University, 5 De Ming Rd., Gui Shan District, Taoyuan City 333, Taiwan, ROC*
[2]*Department of Electrical Engineering, Lunghwa University of Science and Technology, Taoyuan City 333, Taiwan, ROC*
[3]*Department of Electrical Engineering, I-Shou University, No.1, Sec. 1, Syuecheng Rd., Dashu District, Kaohsiung City 84001, Taiwan, ROC*

Received 18 November 2024; Received in revised form 18 February 2025; Accepted 6 March 2025

Abstract

Magnesium titanate ($MgTiO_3$) and calcium lanthanum titanate ($Ca_{0.61}La_{0.26}TiO_3$) are widely regarded as functional ceramic materials with distinct dielectric and structural properties. This study investigates the mixed-phase formation of these two materials in (1-x)$MgTiO_3$–x$Ca_{0.61}La_{0.26}TiO_3$ composites (x = 0.05, 0.1, 0.15 and 0.2), focusing on their microstructural evolution, dielectric properties and phase transition behaviour. The microstructural characteristics of the mixed-phase materials were analysed at different compositional ratios through X-ray diffraction, scanning electron microscopy and dielectric measurements. Furthermore, dielectric testing demonstrated that the mixed-phase materials exhibit enhanced dielectric properties, including higher dielectric constants (ε_r) and more stable temperature characteristics, compared to the individual components. These properties were shown to be dependent on the $MgTiO_3$/$Ca_{0.61}La_{0.26}TiO_3$ ratio, with an optimal ratio offering improved performance for potential applications in the microwave devices. In addition, phase transition behaviour was studied over a range of temperatures, highlighting structural transitions that contribute to the thermal stability of the mixed-phase system. The findings suggest that the combination of $MgTiO_3$ and $Ca_{0.61}La_{0.26}TiO_3$ offers a promising route for developing advanced dielectric materials with tailored properties for specific industrial and technological applications.

Keywords: *$MgTiO_3$, $Ca_{0.61}La_{0.26}TiO_3$, microwave, dielectric properties, dielectric ceramics*

I. Introduction

Dielectric ceramics have significantly contributed to 5G communication systems in last five years, especially in antenna design and RF devices. Dielectric resonator antennas (DRA) have become crucial for 5G due to their low conductive losses and design flexibility, with a focus on compact, multilayer DRAs for millimetre-wave bands using low-temperature co-fired ceramics (LTCC). Microwave dielectric ceramics, like MgO-based composites, improve miniaturized filters and resonators by enhancing dielectric properties and reducing high- frequency losses. Substrate materials like MgO provide low-loss and high thermal stability, while ceramic-based capacitors and resonators enhance quality factors and frequency stability [1–3].

Magnesium titanate ($MgTiO_3$), an ilmenite-based material, is well-known for its high *Q*-factor and low dielectric constant. Recent research on $MgTiO_3$ dielectric ceramics has focused on enhancing microwave properties through various strategies. Cation substitution, such as with Zn^{2+} and Sn^{4+}, has improved quality factors. Novel architectures, including tri-layer co-fired structures using $Li_2Ti_{0.85}(Mg_{1/3}Nb_{2/3})_{0.15}O_3$/$MgTiO_3$ and $MgTiO_3$/TiO_2/$MgTiO_3$ systems, have demonstrated high Qf values and suitable temperature stability. Composite systems, like $MgTiO_3$ with CaO-B_2O_3-SiO_2, have shown enhanced dielectric and mechanical properties for LTCC applications. Doping strategies, such as

*Corresponding author: +886 7 6577711 ext. 6638
e-mail: *ptl@isu.edu.tw*

MgF_2 addition, have significantly improved *Qf* factors. Temperature stability has been addressed through the integration of $(Ca_{0.8}Sr_{0.2})TiO_3$ as a τ_f compensator. Phase control studies in $(1\text{-}x)MgTiO_3$–$x(Mg_4Ta_2O_9)_{1/3}$ ceramics have provided insights into Raman modes and dielectric properties. These advancements are crucial for developing materials suitable for modern wireless communication technologies, particularly 5G applications [4–9].

In contrast, $Ca_{0.61}La_{0.26}TiO_3$, a modified version of $CaTiO_3$ doped with lanthanum, exhibits significantly higher dielectric permittivity and thermal stabile tunability. This makes it more suitable for energy storage applications, high-frequency multilayer ceramic capacitors (MLCCs) and tuneable dielectric devices. By introducing lanthanum into the calcium titanate lattice, the material experiences enhanced dielectric properties, particularly its capacity to sustain higher electrical fields and dielectric tunability under varying voltage conditions. This makes $Ca_{0.61}La_{0.26}TiO_3$ an attractive material for electronic applications that require adjustable capacitance or resonance [10,11]. In our previous research, we enhanced the dielectric properties of $Ca_{0.61}La_{0.26}TiO_3$ by optimizing the calcination conditions (temperature and holding time), resulting in approximately a 5% increase in ε_r, a 10% improvement in the *Qf* value and a 1.7% adjustment in τ_f [12].

The potential for combining $MgTiO_3$ and $Ca_{0.61}La_{0.26}TiO_3$ into a mixed-phase system introduces the exciting possibility of creating a new dielectric material class. This class could balance high dielectric performance and thermal stability, which is crucial for high-performance electronic components. The resulting composite material could possess a unique set of dielectric characteristics optimized for advanced electronic, telecommunication and capacitor technologies. This potential impact on these key industries underscores the practical relevance of the research. Mixed-phase ceramic systems have long been a topic of interest within materials science due to their ability to tailor material properties through compositional tuning. By adjusting the ratio of different phases, it is possible to create materials with hybrid properties that exceed the performance of their components [13–15]. In the case of $MgTiO_3$ and $Ca_{0.61}La_{0.26}TiO_3$, the microstructure of the mixed-phase materials will play a pivotal role in dictating their dielectric and thermal behaviours. Grain size, grain boundary distribution and phase compatibility will all influence the overall performance of the composite material.

II. Experimental

2.1. Sample preparation

Synthesis of the mixed-phase ceramic material composed of magnesium titanate ($MgTiO_3$) and calcium lanthanum titanate ($Ca_{0.61}La_{0.26}TiO_3$) was carried out through a controlled and systematic process to ensure optimal phase distribution and desired dielectric properties. High-purity powders of MgO (96.5%, Showa), TiO_2 (99%, Acros), $CaCO_3$ (99%, Showa) and La_2O_3 (99.9%, Showa) were selected as precursors. Stoichiometric ratios were calculated to synthesize $MgTiO_3$ and $Ca_{0.61}La_{0.26}TiO_3$. For $MgTiO_3$, a 1:1 molar ratio of MgO to TiO_2 was used, while for $Ca_{0.61}La_{0.26}TiO_3$, the appropriate molar ratio of $CaCO_3$, La_2O_3 and TiO_2 was employed to form the doped perovskite structure. The calculated amounts of MgO, TiO_2, $CaCO_3$ and La_2O_3 powders were thoroughly mixed using ball milling for 24 h to ensure uniform distribution and intimate contact between the different particles. The mixed powders were dried and subjected to calcination at 1100 °C for 4 h to initiate the formation of $MgTiO_3$ and $Ca_{0.61}La_{0.26}TiO_3$ phases. The calcined powders were then crushed and sieved to break up any agglomerates. The calcined $MgTiO_3$ and $Ca_{0.61}La_{0.26}TiO_3$ powders were weighed in desired proportions and re-mixed using ball milling or high-energy mixing for further homogenization. The mixed powder was compacted into cylindrical pellets using a uniaxial press at 200 MPa. The pellets were sintered at temperatures between 1350 and 1450 °C for 4 h to achieve densification and complete phase formation.

2.2. Characterization

The sintered samples were characterized to verify phase formation, analyse microstructure and evaluate dielectric properties. X-ray diffraction (XRD, Siemens D5000, Munich, Germany) was performed to confirm the formation of $MgTiO_3$ and $Ca_{0.61}La_{0.26}TiO_3$ phases and to check for any unwanted secondary phases. Scanning electron microscopy (SEM, Philips XL-40FEG, Eindhoven, the Netherlands) was used to observe the microstructure, grain size and grain boundary distribution. Energy dispersive X-ray spectroscopy (EDS) was employed to analyse the elemental composition of the sample. The dielectric properties, including the dielectric constant (ε_r) and quality factor (*Qf*), were measured using a network analyser operating within microwave frequency ranges. The temperature coefficient of resonant frequency (τ_f) was determined by tracking the resonant frequency over a temperature range from 25 to 85 °C [16–18]. The apparent density of the sintered ceramics was measured using the Archimedes method to ensure accuracy in correlating density with dielectric performance.

III. Results and discussion

The XRD analysis of the mixed-phase ceramics comprising $MgTiO_3$ and $Ca_{0.61}La_{0.26}TiO_3$, as shown in Figs. 1 and 2, reveals distinct diffraction peaks for both primary phases, confirming their coexistence in the composites. The $MgTiO_3$ phase exhibits characteristic peaks at 2θ angles of 24.5° (104), 33.2° (110) and 32.8° (211), consistent with the JCPDS #06-0494 reference. Sim-

ilarly, the $Ca_{0.61}La_{0.26}TiO_3$ phase shows reflections at 2θ angles of 32.5° (200)/(121) and 46.5° (220), consistent with the JCPDS #42-0423 reference. Peak indexing was performed based on the dominant phases identified from XRD analysis. In Figs. 1 and 2, the diffraction peaks are primarily assigned based on the dominant $MgTiO_3$ phase. However, certain peaks may have overlapping contributions from $Ca_{0.61}La_{0.26}TiO_3$. In particular, the peak observed around 32–33°, which has been indexed as $MgTiO_3$ (211), coincides with the expected positions of $Ca_{0.61}La_{0.26}TiO_3$ (200)/(121). In addition to the primary phases, some minor peaks corresponding to secondary phases were observed. The secondary phase, identified as $MgTi_2O_5$, exhibits characteristic diffraction peaks at 2θ angles of 26.0°, 38.9° and 41.5°, consistent with the ICDD #35-0792 reference [19–23]. While the peak at 26.0° is primarily associated with $MgTi_2O_5$, we acknowledge that $Ca_{0.61}La_{0.26}TiO_3$ (111) may also contribute to this diffraction signal. However, the presence of additional peaks at 38.9° and 41.5°, which do not overlap with $Ca_{0.61}La_{0.26}TiO_3$, further confirms the formation of $MgTi_2O_5$. This secondary phase may result from slight deviations in stoichiometry or incomplete reactions during synthesis. Figure 1 confirms that with the increase in sintering temperature, the $MgTi_2O_5$ phase gradually forms, especially in the samples sintered at 1425 and 1450 °C, where its content progressively increased. The $MgTiO_3$ phase remains relatively stable at all temperatures. Figure 2 shows that as the x value (the content of $Ca_{0.61}La_{0.26}TiO_3$) increases, the diffraction peaks of the $Ca_{0.61}La_{0.26}TiO_3$ phase become progressively stronger, while the diffraction peaks of the $MgTiO_3$ phase relatively weaken. The $MgTi_2O_5$ phase gradually forms as the x value increases. The proportion of $MgTiO_3$ and $Ca_{0.61}La_{0.26}TiO_3$ changes and the relative intensities of these peaks also shift, indicating a variation in the phase composition with different mixing ratios.

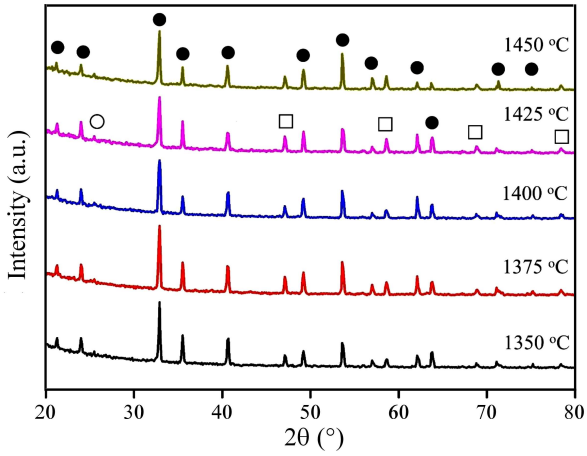

Figure 1. XRD results of $0.85MgTiO_3$–$0.15Ca_{0.61}La_{0.26}TiO_3$ ceramics at different sintering temperatures (● - $MgTiO_3$, □ - $Ca_{0.61}La_{0.26}TiO_3$, ○ - $MgTi_2O_5$)

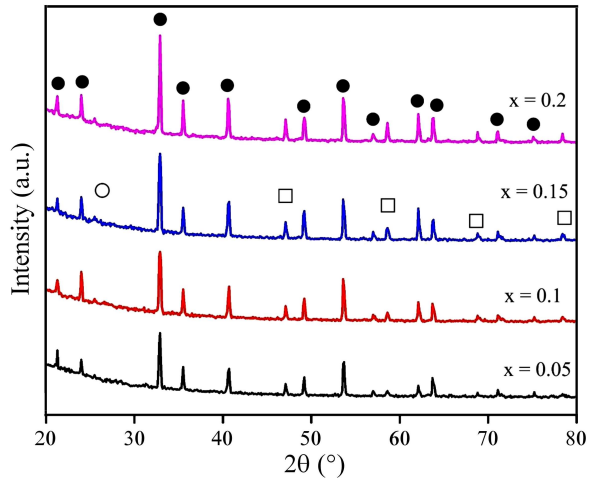

Figure 2. XRD results of $(1-x)MgTiO_3$–$xCa_{0.61}La_{0.26}TiO_3$ ceramics at their optimum sintering temperatures for various x values

Tables 1 and 2 present the calculated lattice constants and phase contents for each component. In both tables, the lattice parameters a and c are associated with the dominant $MgTiO_3$ phase, which exhibits $R\bar{3}$ rhombohedral symmetry. Given that $MgTiO_3$ constitutes the majority phase in the mixed-phase system, the lattice parameters listed in these tables reflect the structural characteristics of $MgTiO_3$. The lattice parameters for $MgTiO_3$ align well with the expected values, confirming successful phase formation. However, the presence of secondary phases, although limited in percentage, could impact the overall dielectric properties of the material. These secondary phases may introduce additional dielectric loss or alter the effective permittivity, potentially degrading the performance of the composite in applications where precise dielectric behaviour is required. Consequently, further optimization of the synthesis process may be necessary to minimize the formation of these secondary phases and achieve optimal dielectric characteristics. The variation in phase per-

Table 1. Lattice parameters and compositions of $0.85MgTiO_3$–$0.15Ca_{0.61}La_{0.26}TiO_3$ ceramics sintered at various temperatures for 4 h (phase contents were determined by calculating the relative peak areas of each phase from the XRD results)

Sintering temperature [°C]	$MgTiO_3$ lattice parameters		$MgTiO_3$ content [mol%]	$Ca_{0.61}La_{0.26}TiO_3$ content [mol%]	$MgTi_2O_5$ content [mol%]
	a [nm]	c [nm]			
1350	0.5046 ± 0.00072	1.3872 ± 0.00292	85.7	9.0	5.3
1375	0.5048 ± 0.00088	1.3867 ± 0.00354	84.1	11.2	4.7
1400	0.5046 ± 0.00072	1.3872 ± 0.00292	85	9.6	5.4
1425	0.5048 ± 0.00088	1.3867 ± 0.00354	82.4	12.1	5.4
1450	0.5048 ± 0.00088	1.3867 ± 0.00354	83	11.5	5.5

Table 2. Lattice parameters and phase compositions of (1-*x*)$MgTiO_3$–*x*$Ca_{0.61}La_{0.26}TiO_3$ ceramics sintered at 1400 °C for 4 h

x value	$MgTiO_3$ lattice parameters		$MgTiO_3$ content [mol%]	$Ca_{0.61}La_{0.26}TiO_3$ content [mol%]	$MgTi_2O_5$ content [mol%]
	a [nm]	*c* [nm]			
0.05	0.5046 ± 0.00072	1.3872 ± 0.00292	85.7	8.1	6.2
0.10	0.5046 ± 0.00072	1.3872 ± 0.00292	85.4	8.9	5.7
0.15	0.5046 ± 0.00072	1.3872 ± 0.00292	85	9.6	5.4
0.20	0.5048 ± 0.00088	1.3867 ± 0.00354	84	11.1	4.9

centages also influences the material's structural and dielectric characteristics. A higher proportion of $MgTiO_3$ may enhance densification and structural stability, while a higher $Ca_{0.61}La_{0.26}TiO_3$ content could significantly increase dielectric constant, but with the trade-off of increased amount of secondary phases. This composition-dependent behaviour highlights the importance of optimizing the phase ratio to balance desired dielectric properties with phase purity and structural integrity.

SEM analysis of the mixed-phase ceramics comprising $MgTiO_3$ and $Ca_{0.61}La_{0.26}TiO_3$, as shown in Figs. 3 and 4, reveals a microstructure where $MgTiO_3$ forms larger, irregularly shaped grains. At the same time, $Ca_{0.61}La_{0.26}TiO_3$ exhibits smaller, well-defined square-shaped grains. These distinct morphologies are visible, with the larger $MgTiO_3$ grains dominating certain regions and the smaller, well-defined $Ca_{0.61}La_{0.26}TiO_3$ grains interspersed throughout the structure. The well-defined grain boundaries suggest limited interaction between the two phases.

Notable grain size and morphology changes are observed in both phases with the increase of sintering temperature (Fig. 3). The grain growth is less pronounced at lower sintering temperature and the corresponding microstructure is characterized with smaller $MgTiO_3$ grains as well as more tightly packed $Ca_{0.61}La_{0.26}TiO_3$ grains (Fig. 3a). However, as the sintering temperature rises, the $MgTiO_3$ grains significantly increase in size (Fig. 3c). In contrast, $Ca_{0.61}La_{0.26}TiO_3$ grains retain their square shape but slightly increase in size, leading to a more heterogeneous microstructure. The grain boundary density decreases at higher sintering temperatures due to the enhanced grain growth, especially for $MgTiO_3$. This can improve densification, but may also introduce more significant variations in grain size, potentially leading to the localized stress and inhomogeneities within the material. The influence of $Ca_{0.61}La_{0.26}TiO_3$ on the composite microstructure is shown in Fig. 4. The ceramics with higher amount of $Ca_{0.61}La_{0.26}TiO_3$ phase (Fig. 4c) has more homogeneous microstructure with smaller grain sizes.

In addition to these primary phases, a small fraction of elongated grains is observed, particularly at higher sintering temperatures, and are identified as secondary phase ($MgTi_2O_5$), as highlighted in Fig. 5 (spot C). These secondary elongated grains could impact the overall dielectric properties of the ceramics by introducing inhomogeneities and affecting the grain boundary behaviour. The observed changes in grain size and morphology at different sintering temperatures could significantly influence the material's dielectric properties, particularly in permittivity and dielectric loss, underlining the potential impact of our research on the performance of these materials.

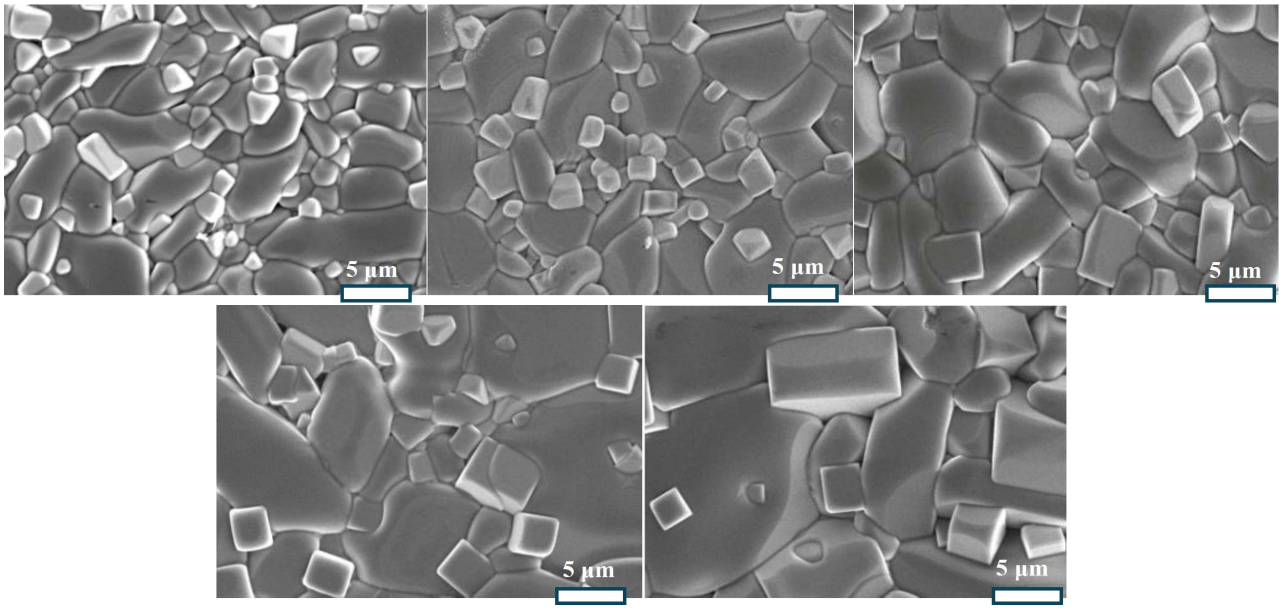

Figure 3. SEM images of 0.85$MgTiO_3$–0.15$Ca_{0.61}La_{0.26}TiO_3$ ceramics sintered at various temperatures: a) 1350 °C, b) 1375 °C, c) 1400 °C, d) 1425 °C and e) 1450 °C for 4 h

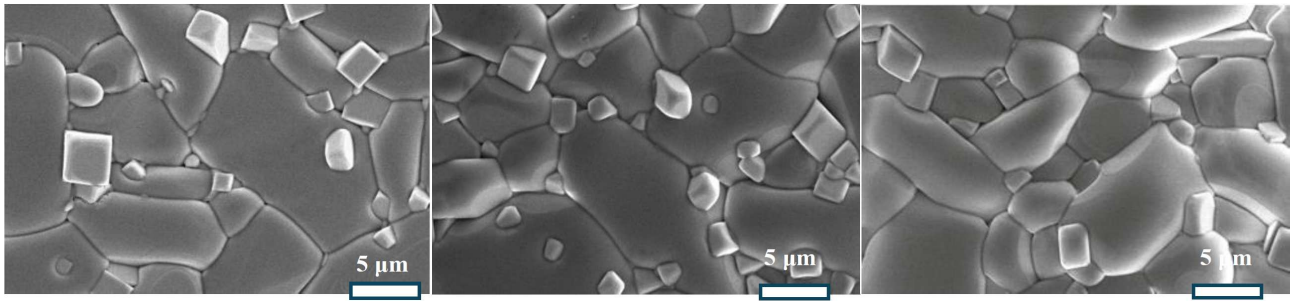

Figure 4. SEM images of (1-x)$MgTiO_3$–$xCa_{0.61}La_{0.26}TiO_3$ ceramics (sintered at 1400 °C for 4 h) with different compositions: a) x = 0.05, b) x = 0.1 and c) x = 0.2

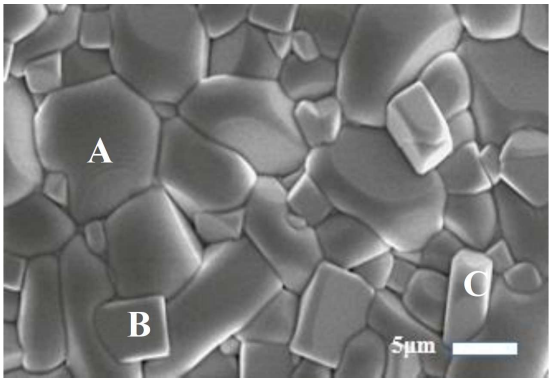

Content	Spot A	Spot B	Spot C
Mg [at.%]	19.80	0	12.14
Ca [at.%]	0	11.01	0
La [at.%]	0	5.34	0
Ti [at.%]	18.75	20.53	25.60
O [at.%]	61.45	63.12	62.26

Figure 5. SEM image (a) and corresponding EDS results (b) of 0.85$MgTiO_3$–0.15$Ca_{0.61}La_{0.26}TiO_3$ ceramics

Although secondary phases like $MgTi_2O_5$ were observed, their content remained minimal under optimized conditions. Recent literature suggests that these secondary phases can introduce additional dielectric loss. However, their impact was mitigated by carefully controlling the sintering parameters in this study. Additional insights from referenced works align with our findings, indicating that porosity and grain interaction play a significant role in determining the dielectric properties of mixed-phase ceramics.

To better understand the elemental composition and distribution within these phases, the EDS analysis was performed (Fig. 5). The EDS results confirm that Mg is predominantly localized within the larger $MgTiO_3$ grains (spot A). In comparison, Ca and La are concentrated in the smaller $Ca_{0.61}La_{0.26}TiO_3$ grains (spot B). The rod-like grains (spot C) are identified as $MgTi_2O_5$. Titanium is distributed uniformly across both phases, as expected. In summary, the microstructural evolution with increasing sintering temperature includes the formation of a small fraction of elongated secondary phase grains, as confirmed by SEM and EDS analyses (Fig. 5). These secondary phases, particularly the elongated grains identified as $MgTi_2O_5$, could play a significant role in determining the composite material's final dielectric and structural properties, highlighting the importance of our findings in understanding the behaviour of these materials.

The density (ρ) and dielectric constant (ε_r) of the mixed-phase ceramics comprising $MgTiO_3$ and $Ca_{0.61}La_{0.26}TiO_3$ (Fig. 6a and Table 3) demonstrate a strong dependence on both the sintering temperature and the phase ratio. As the sintering temperature increases, there is a notable improvement in densification, particularly in compositions with a higher $MgTiO_3$ content. This is reflected in the higher density values at elevated temperatures, where the larger grains of $MgTiO_3$ contribute to better packing and reduced porosity. Conversely, the $Ca_{0.61}La_{0.26}TiO_3$ phase, with its smaller, square-shaped grains, tends to retain more porosity at lower sintering temperatures, leading to a slightly lower density. To account for the impact of porosity on dielectric properties, the relative density (ρ_{rel}) was calculated from the measured (ρ_{meas}) and theoretical (ρ_{th}) densities using the following equation:

$$\rho_{rel} = \frac{\rho_{meas}}{\rho_{th}} \times 100 \quad (1)$$

The computed relative density values are presented in Fig. 6b. It is observed that relative density increases with sintering temperature, reaching a peak at 1400 °C, which is consistent with the optimal densification, observed in SEM micrographs. Regarding the dielectric constant (ε_r), the results vary with both sintering temperature and phase ratio. $MgTiO_3$, known for its lower dielectric constant, provides stability and moderates the overall ε_r of the composite. As shown in Fig. 6a, when the proportion of $Ca_{0.61}La_{0.26}TiO_3$ increases, the dielectric constant rises significantly due to its inherently higher ε_r. The ability to adjust the $MgTiO_3$/$Ca_{0.61}La_{0.26}TiO_3$ ratio provides flexibility in tuning the dielectric properties of the material for specific applications. Furthermore, the sintering temperature is critical for microstructural evolution and dielec-

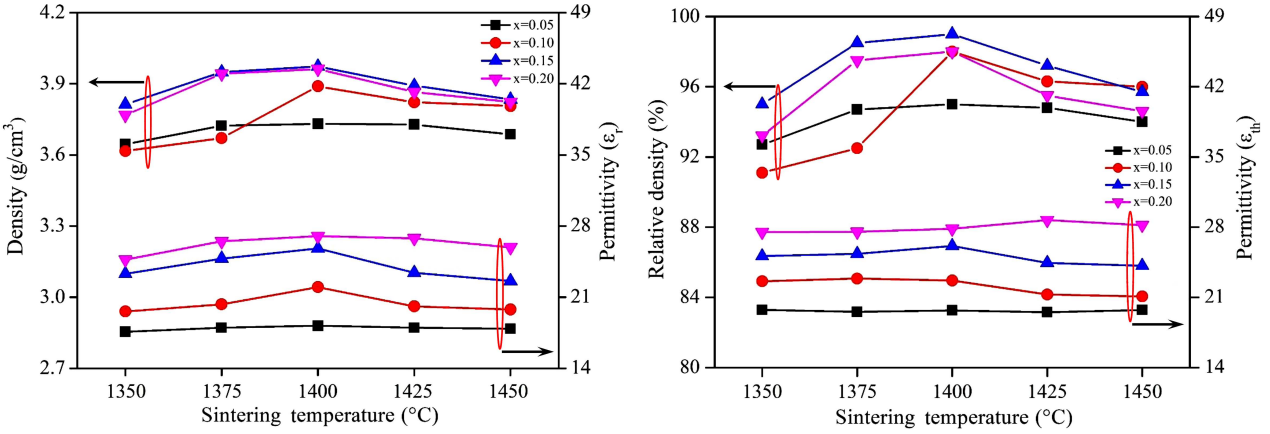

Figure 6. Apparent density and measured dielectric constant (a) and relative density and theoretical dielectric constant, ε_{th} (b) of (1-x)$MgTiO_3$–$xCa_{0.61}La_{0.26}TiO_3$ ceramics as functions of sintering temperature

Table 3. The dielectric performances with various x values for (1-x)$MgTiO_3$–$xCa_{0.61}La_{0.26}TiO_3$ ceramics sintering at 1400 °C

x values	ρ [g/cm^3]	ε_r	Qf [GHz]	τ_f [ppm/°C]
0.05	3.73	18.2	131900	−27.8
0.10	3.89	22	115300	−11.9
0.15	3.97	25.8	108000	−0.8
0.20	3.96	27	72500	−11 9

tric performance. At lower sintering temperatures, incomplete densification leads to higher porosity, reducing the density and dielectric constant. As the sintering temperature increases, grain growth is enhanced, particularly for $MgTiO_3$, resulting in a denser material with improved dielectric properties. However, excessively high sintering temperatures can lead to the formation of secondary phases, as identified in the SEM and EDS analyses, which can introduce dielectric losses and lower overall performance. Thus, the optimal balance between sintering temperature and phase ratio is crucial for achieving desired material properties.

Furthermore, the dielectric constant was corrected for porosity using the empirical formula [24,25]:

$$\varepsilon_{th} = \frac{\varepsilon_{meas}}{1 - 1.5p} \tag{2}$$

where $p = 1 - \rho_{rel}$ represents the porosity fraction derived from relative density. The corrected dielectric constant values, presented in Fig. 6b, demonstrate a more systematic trend with sintering behaviour, reinforcing the direct influence of porosity on dielectric performance. These corrections were incorporated into our analysis to provide a more accurate evaluation of the relationship between densification and dielectric properties. Higher $MgTiO_3$ content and appropriate sintering conditions enhance densification while increasing the $Ca_{0.61}La_{0.26}TiO_3$ proportion can elevate the dielectric constant. However, the secondary phases at higher temperatures necessitate careful control to minimize adverse effects on density and dielectric properties. Figure 6b clearly illustrates these trends, highlighting the complex interplay between phase composition, sintering temperature and material characteristics.

The quality factor (Qf value) and temperature coefficient (τ_f value) for the mixed-phase ceramics comprising $MgTiO_3$ and $Ca_{0.61}La_{0.26}TiO_3$ are critical parameters for evaluating its suitability in dielectric applications. As illustrated in Fig. 7, the results demonstrate that Qf values generally improve with increasing $MgTiO_3$ content attributable to its lower dielectric losses compared to $Ca_{0.61}La_{0.26}TiO_3$. The larger, more uniform grains of $MgTiO_3$ contribute to the reduced scattering and grain boundary losses, leading to higher Qf values, as depicted in Fig. 7 [26,27]. The maximum Qf value observed at 1400 °C, rather than 1450 °C, can be explained by the formation of secondary phases at higher sintering temperatures. At 1400 °C, the material achieves optimal densification and grain growth, leading to reduced dielectric losses and higher Qf values. Moreover, at 1450 °C, the increased formation of secondary phases, such as $MgTi_2O_5$, introduces additional dielectric losses and grain boundary scattering. These secondary phases disrupt the homogeneity of the microstructure and increase dielectric losses, resulting in

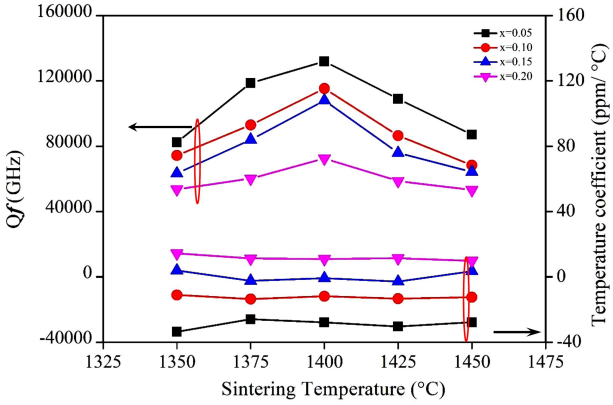

Figure 7. Qf and τ_f values of (1-x)$MgTiO_3$–$xCa_{0.61}La_{0.26}TiO_3$ ceramics with various x values and sintering at varied temperatures

lower *Qf* values. This behaviour is consistent with recent studies, which have reported that excessive sintering temperatures can lead to the formation of undesirable secondary phases and degrade the dielectric performance of ceramics [28,29].

Conversely, the τ_f values reflect the stability of the dielectric performances with temperature changes. As shown in Fig. 7, τ_f tends to become more stable with an increase in $Ca_{0.61}La_{0.26}TiO_3$ content. This stability arises from the enhanced structural characteristics provided by the $Ca_{0.61}La_{0.26}TiO_3$ phase, which helps to mitigate the dielectric variations commonly associated with temperature fluctuations. The high ionic mobility and polarizability of $Ca_{0.61}La_{0.26}TiO_3$ contribute to a more uniform dielectric response across a range of temperatures, resulting in improved overall performance of the composite. This enhanced temperature stability is advantageous for applications where consistent dielectric behaviour is crucial, making incorporating $Ca_{0.61}La_{0.26}TiO_3$ a beneficial strategy in optimizing the material's dielectric properties. Furthermore, secondary phases ($MgTi_2O_5$) significantly impact *Qf* and τ_f values. The formation of these secondary phases, especially at elevated sintering temperatures, can introduce additional dielectric losses and alter the overall dielectric response of the material. These secondary phases often lead to increased grain boundary scattering and a less homogeneous microstructure, which can diminish the *Qf* and destabilize the τ_f values. Their presence complicates the dielectric characteristics, making it crucial to carefully control sintering conditions to minimize their formation.

The influence of sintering temperature on both *Qf* and τ_f is also significant. Increased sintering temperatures generally enhance densification and grain growth, improving *Qf* values. Higher temperatures allow for better particle interconnection and reduced porosity, reducing dielectric losses. However, excessively high sintering temperatures may facilitate the development of secondary phases, which can compromise *Qf* and τ_f. The interplay between *Qf* values and τ_f highlights the trade-offs involved in optimizing the mixed-phase ceramics' properties. While higher $MgTiO_3$ content enhances *Qf* values by reducing losses, an increase in $Ca_{0.61}La_{0.26}TiO_3$ leads to more significant dielectric variability with temperature, which could compromise performance in temperature-sensitive applications. Therefore, achieving an optimal balance between these properties is crucial for developing materials with desirable dielectric characteristics. Overall, as illustrated in Fig. 7, the findings underscore the importance of carefully tuning the phase composition and processing conditions to enhance the mixed-phase ceramics' quality factor and temperature stability, ensuring its viability for various electronic applications. This balance will ultimately determine the suitability of the material for specific applications where high performance and stability are required.

To validate our findings, the dielectric constant (ε_r) values were compared with the literature on similar ceramics. Ma *et al.* [30] reported ε_r values of 16–18 for $MgTiO_3$ ceramics with glass additions, aligning with our high-$MgTiO_3$ compositions. Rabha *et al.* [31] found increasing the secondary phase in (1-*x*)$MgTiO_3$–*x*$SrTiO_3$ raised ε_r, consistent with our results for higher $Ca_{0.61}La_{0.26}TiO_3$ content. Variations in ε_r arise from phase composition, sintering conditions, and microstructure. Secondary phases like $MgTi_2O_5$ may also influence dielectric losses. These comparisons confirm that our results align with prior studies, supporting the reliability of our analysis [30,31].

IV. Conclusions

This study systematically investigates the dielectric properties, microstructure and phase evolution of mixed-phase $MgTiO_3$–$Ca_{0.61}La_{0.26}TiO_3$ ceramics. The results demonstrate that increasing $MgTiO_3$ content enhances the quality factor (*Qf*) due to its lower dielectric losses, while $Ca_{0.61}La_{0.26}TiO_3$ incorporation stabilizes τ_f, ensuring thermal reliability. To better understand the relationship between porosity and dielectric behaviour, relative density calculations and dielectric constant corrections were applied. The corrected theoretical dielectric constant (ε_{th}) exhibits a systematic trend with densification, reinforcing the role of microstructural evolution. The results confirm that optimizing sintering conditions enhances density and dielectric performance. Additionally, the formation of $MgTi_2O_5$ at elevated temperatures has negative impact on *Qf*, not only due to its presence but also due to its morphological evolution. SEM and EDS analyses indicate that changes in $MgTi_2O_5$ distribution contribute to the increased dielectric losses, highlighting the importance of controlling secondary phase formation. A balanced $MgTiO_3$/$Ca_{0.61}La_{0.26}TiO_3$ ratio, combined with optimized sintering conditions, leads to the superior dielectric performance, making these ceramics promising candidates for dielectric applications.

Acknowledgement: This work was supported by the I-Shou University under grant ISU-112-IUC-02.

References

1. M.D. Hill. D.B. Cruickshank, I.A. MacFarlane, "Perspective on ceramic materials for 5G wireless communication systems", *Appl. Phys. Lett.*, **118** (2021) 120501.
2. S. Zhu, Z. Huang, W. Lou, K. Song, A. Khesro, F. Hussain, Z. Tan, X. Luo, M. Mao, L. Xue, P. Xu, B. Liu, H. Lin, D. Wang, "5G microstrip patch antenna and microwave dielectric properties of 4 mol% LiF-MgO-*x*wt% $MTiO_3$ (M = Ca, Sr) composite ceramics", *J. Mater. Sci. Mater. Electron.*, **32** (2021) 23880–23888.
3. Y. Zhang, S. Ogurtsov, V. Vasilev, A.A. Kishk, D. Caratelli, "Advanced dielectric resonator antenna technology for 5G and 6G applications", *Sensors*, **24** (2024) 1413.
4. L.X. Li, X.R He, T. Yue, Y. Zhan, M.K. Du,

"$L_2Ti_{0.85}(Mg_{1/3}Nb_{2/3})_{0.15}O_3$/$MgTiO_3$/$L_2Ti_{0.85}(Mg_{1/3}Nb_{2/3})_{0.15}O_3$ tri-layer co-fired microwave dielectric ceramics: A strategy to suppress non-linear variation of resonant frequency with temperature and achieve a high Q value", *Appl. Phys. Lett*., **120** (2022) 222901.

5. J. Zhang, Z. Yue, Y. Luo, L. Li, "$MgTiO_3$/TiO_2/$MgTiO_3$: An ultrahigh-Q and temperature-stable microwave dielectric ceramic through cofired trilayer architecture", *Ceram. Int*., **44** (2018) 21000–21003.
6. X. Zhu, F. Kong, X. Ma, "Sintering behavior and properties of $MgTiO_3$/CaO-B_2O_3-SiO_2 ceramic composites for LTCC applications", *Ceram. Int*., **45** (2019) 1940–1945.
7. Z. Xu, L. Li, S. Yu, M. Du, W. Luo, "Magnesium fluoride doped $MgTiO_3$ ceramics with ultra-high Q value at microwave frequencies", *J. Alloys Compd.*, **802** (2019) 1–5.
8. D. Gui, C. Wang, W. Zhu, C. Meng, "Phase controlled Raman modes and dielectric properties in (1-x)$MgTiO_3$-x$(Mg_4Ta_2O_9)_{1/3}$", *J. Alloys Compd*., **730** (2018) 434–440.
9. J. Iqbal, H. Liu, H. Hao, A. Ullah, M. Cao, Z. Yao, A. Manan, "$Mg(Ti_{0.95}Sn_{30.05})O_3$–$(Ca_{0.8}Sr_{0.2})TiO_3$ ceramics: Phase, microstructure, and microwave dielectric properties", *J. Alloys Compd*., **742** (2018) 107–111.
10. C.H. Shen, C.L. Huang, "A novel temperature-compensated microwave dielectric (1-x)$(Mg_{0.95}Ni_{0.05})TiO_3$-x$Ca_{0.6}La_{0.8/3}TiO_3$ ceramics system", *Int. J. Appl. Ceram. Technol*., **6** [5] (2009) 562–570.
11. C.L. Pan, C.H. Shen, "Tunable microwave dielectric properties of $Ca_{0.6}La_{0.8/3}TiO_3$ and $Ca_{0.8}Sm_{0.4/3}TiO_3$-modified $(Mg_{0.6}Zn_{0.4})_{0.95}Ni_{0.05}TiO_3$ ceramics with a near-zero temperature coefficient", *Molecules*, **26** (2021) 4715.
12. C.H. Shen, C.H. Hu, J.Y. Chen, W.H. Chen, C.W. Tung, Y.H. Yang, T.Y. Yang, "Examining the impact of sintering conditions on the microwave dielectric properties of $Ca_{0.61}M_{0.26}TiO_3$ (M = La^{3+}, Nd^{3+})", *J. Ceram. Process. Res*., **25** [5] (2024) 790–797
13. Y.B. Chen, J. Peng, "Zero-temperature coefficient of resonant Frequency in $[(Mg_{0.6}Zn_{0.4})_{0.95}Co_{0.05}]_{1.02}TiO_{3.02}$ -$Ca_{0.6}(La_{0.9}Y_{0.1})_{0.2667}TiO_3$ ultra-low-loss composite dielectrics", *Ceramics*, **7** [2] (2024) 466–477.
14. C.H. Shen, C.L. Pan, "Dielectric properties and applications of low-loss (1-x)$(Mg_{0.95}Ni_{0.05})_2TiO_4$-x$SrTiO_3$ ceramic system at microwave frequency", *Int. J. Appl. Ceram. Technol*., **12** [S1] (2015) E127–E133.
15. L. Zhang, H. Ren, H.I. Peng, H. Lin, Q. Yang, "Sintering behavior of 0.95$MgTiO_3$-0.05$CaTiO_3$ ceramics with high densification, high Q and enhanced mechanical properties for 5G massive MIMO technology: Effect of particle gradation", *Ceram. Int*., **50** [3] (2024) 4462–4468.
16. B.W. Hakki, P.D. Coleman, "A dielectric resonator method of measuring inductive capacities in the millimeter range", *IEEE Trans. Microwave Theory Tech*., **8** (1960) 402–410.
17. S.B. Cohn, K.C. Kelly, "Microwave measurement of high-dielectric-constant materials" *IEEE Trans. Microwave Theory Tech*., **14** [9] (1966) 406–410.
18. W.E. Courtney, "Analysis and evaluation of a method of measuring the complex permittivity and permeability microwave insulators", *IEEE Trans. Microwave Theory Tech*., **18** (1970) 476–485.
19. Y.-C. Liou, S.-L. Yang, "Calcium-doped $MgTiO_3$-$MgTi_2O_5$ ceramics prepared using a reaction-sintering process", *Mater. Sci. Eng. B*, **142** (2007) 116–120.
20. Y. Nakagoshi, Y. Suzuki, "Dimensional change behavior of porous $MgTi_2O_5$ in reactive sintering", *Ceram. Int*., **43** [6] (2017) 4701–4706.
21. L. He, H. Yu, M. Zeng, E. Li, J. Liu, S. Zhang, "Phase compositions and microwave dielectric properties of $MgTiO_3$-based ceramics obtained by reaction-sintering method", *J. Electroceram*., **40** (2018) 360–364.
22. F.U. Ermawati, "XRD and EDX analyses on the formation of $MgTiO_3$ phase in $(Mg_{0.6}Zn_{0.4})(Ti_{0.99}Sn_{0.01})O_3$ powders due to calcination temperature variations", *J. Phys. Conf. Ser*., **2110** (2021) 012009.
23. H. Li, B. Tang, Y.X. Li, Z.J. Qing, S.R. Zhang, "Effects of $Mg_{2.05}SiO_{4.05}$ addition on phase structure and microwave properties of $MgTiO_3$-$CaTiO_3$ ceramic system", *Mater. Lett*., **145** (2015) 30–33.
24. W. Luo, J. Guo, C. Randall, M. Lanagan, "Effect of porosity and microstructure on the microwave dielectric properties of rutile", *Mater. Lett*., **200** (2017) 101–104.
25. S.J. Penn, N.M. Alford, A. Templeton, X. Wang, M. Xu, M. Reece, K. Schrapel, "Effect of porosity and grain size on the microwave dielectric properties of sintered alumina", *J. Am. Ceram. Soc*., **80** [7] (1997) 1885–1888.
26. G.L. Gurevich, A.K. Tagantsev, "Intrinsic dielectric loss in crystals: Low temperature", *Sov. Phys. JETP*, **64** (1986) 142–151.
27. G.L. Gurevich, A.K. Tagantsev, "Intrinsic dielectric loss in crystals", *Adv. Phys*., **40** (1991) 719–767.
28. Y. Liu, X. Chen, L. Wang, W. Li, H. Zeng, "Dielectric properties, microstructure and phase evolution of non-stoichiometric 0.9Mg_2SiO_4-0.1$CaTiO_3$ microwave dielectric ceramics", *Ceram. Int*., **47** (2021) 24868–24876.
29. M. Wang, Y. Zhang, H. Huang, J. Liu, Z. Zhou, "Effects of Eu^{3+}/Ta^{5+} nonstoichiometric ratio on dielectric properties of $(Eu_xTa_{1-x})_{0.08}Ti_{0.92}O_2$ ceramics with colossal permittivity: Experiments and first-principle calculations", *Ceram. Int*., **47** (2021) 33798–33804.
30. J.-L. Ma, X. Zhang, Y. Chen, L. Wang, "Effect of glass additions on sintering behavior and dielectric properties of $MgTiO_3$ ceramics", *Integr. Ferroelectr*., **231** [1] (2023) 126–132.
31. S. Rabha, A. Dutta, P. Nath, "Structural, electrical properties and stability in microwave dielectric properties of (1-x)$MgTiO_3$-x$SrTiO_3$ composite ceramics", *J. Alloys Compd*., **875** (2021) 159726.